Received: 18 August 2025 | Accepted: 12 February 2026

DOI: 10.1111/2041-210x.70277

Methods in Ecology and Evolution

RESEARCH ARTICLE

ALTAA: Analysis of long-term activity patterns in ant colonies

Jinook Oh[1,2] | **Sylvia Cremer**[1]

[1]ISTA (Institute of Science and Technology Austria), Klosterneuburg, Austria

[2]Acoustics Research Institute, Austrian Academy of Sciences, Vienna, Austria

Correspondence
Jinook Oh
Email: jinook0707@gmail.com; jinook.oh@oeaw.ac.at

Funding information
European Research Council (ERC) under the European Union's Horizon 2020 Research and Innovation Programme, Grant/Award Number: 771402

Handling Editor: Graziella Iossa

Abstract

1. Collective behaviours are a fascinating study area due to the emergent properties that can only arise in groups of interacting individuals. However, their quantitative study is often impaired by technical difficulties, creating either low-quality and sparse data or impractical data amounts, particularly when capturing large groups over long periods of time. Common challenges arise from recording group members with as little obscuring of each other as possible, as well as in generating manageable data amounts with as high as possible information content.
2. We here provide a multicomponent system that allows to record, analyse and simulate the long-term spatiotemporal activity patterns of insect collectives, especially ant colonies. Our Ant Observing System, ALTAA, comprises a flat-nest design to prevent occlusion of individuals, a recording system running on a low-power single-board-computer, and a set of computer programmes performing quantitative analyses to guide the formation and validation of rules underlying the observed collective patterns. Our system is scalable in that it allows parallel, continuous observation of a high number of colonies using low memory space, with colony maintenance requirements (e.g. feeding, nest humidity) being achieved at lowest possible disturbance by the experimenter.
3. We showcase the potential of the system in a study using the black garden ant, *Lasius niger*, where we analyse the spatiotemporal effects of different group sizes (1, 6, 10 ants), brood (larvae) presence or absence, as well as of different nest geometries, over a period of 1 week. We show that the ants' motion activity has a weak periodicity in the range of 20 to 120 min promoted by larval presence, and that ants are spatially attracted to their larvae, the water source and the walls. We also find that the presence of nestmates lowers an individual ant's motion activity. Observed data are compared to simulations of the temporal activity of the ants.
4. ALTAA provides a powerful toolkit to quantify and interpret spatial and temporal collective activity patterns in (social) insects over extended periods.

KEYWORDS
ant behaviour, behaviour observation, computer-aided ethology, open-source system

1 | INTRODUCTION

Social insects express a diversity of collective actions and behavioural changes in response to diverse stimuli they receive. In many cases, behaviours occur instantaneously as a clearly noticeable reaction to stimulus exposure, such as, for example, the immediate attack of an intruder to their nest (Bhatkar et al., 1972; Phillips & Willis, 2005; Scharf et al., 2011), necrophoric behaviour to remove corpses (Wilson et al., 1958), or sanitary care of pathogen-exposed colony members (Cremer, 2019; Currie & Stuart, 2001; Theis et al., 2015). These clear behavioural reactions can be studied experimentally upon presenting the respective stimulus and observing the insects' reaction. This approach has frequently been used to provide detailed observational data of a relatively low number of individuals or events, to describe the insects' behavioural repertoire and its dependency on triggers. In addition, a whole-colony approach can be used to study how different stimuli change the social interaction networks of colonies (Boenisch et al., 2018; Geffre et al., 2020; Mersch et al., 2013; Stroeymeyt et al., 2018) or their spatial usage (Quevillon et al., 2015; Theraulaz et al., 2002). Here, a common approach is to tag each individual group member before the experiment, by either RFID tags, colour coding or ARtags (Boenisch et al., 2018; Gal et al., 2020; Geffre et al., 2020; Mersch et al., 2013; Pull et al., 2018; Robinson et al., 2009; Stroeymeyt et al., 2018) and to follow the location of each individual over time. Individual tagging requires a lot of resources both during and after the experiment, yet it overcomes issues in social insect tracking—less prominent in less social species—in that their very close social interactions often lead to occlusion of individuals, introducing the constant need for differentiation of individuals during and after their social interaction. Social insects are thus 'too social' for the application of many conventional trackers developed for, for example, flies, fish or mice (Ardekani et al., 2013; Castelo et al., 2020; Giancardo et al., 2013; Liu et al., 2023; Miller et al., 2022), particularly when observed in experimental nest boxes with larger empty space than their natural nests, which are, in the case of ants, often tight underground tunnel and chamber systems (Hölldobler & Wilson, 1990). We therefore implemented a tight nest space which allows the ants to move normally but constrains crawling on top of each other, to facilitate less resource-intense long-term observation of their activity without the need for individual tagging. Such methods are particularly valuable for research questions that do not require individual identity information but focus on the emergence of collective activity patterns in time and space. These can be analysed by, for example, motion measures, as used in the analysis of collective phenomena (Kays et al., 2022; Papadopoulou et al., 2023; Young et al., 2000). It requires considerably less memory space so that even long-term observations over multiple weeks produce data quantities manageable for human analysis. Upscaling data size and managing it using combinations of non-linear computational units is needed to recognize complex patterns, however it often processes the data in a difficult way to be interpreted by humans. Both methods for investigating interactions among individuals and the global pattern of the group are required to understand a complex biological system. A further advantage of tag-free systems for long-term observations is that they are disturbance-free, are not affected by tag-loss issues and allow for birth and dead in the colony, hence allowing for studies of colony development. Most importantly—and other than the study of specific reactions to a particular trigger or of social interaction networks—these analyses can also be performed in the absence of one-on-one interactions and the expression of particular behaviours and hence can capture a greater variety of activity patterns, including also more subtle changes within a noisy background. They hereby benefit from simultaneously extracting information of a high number of colony members (though they also can be used for the observation of individuals), over a long time-span and a potentially large nest area. Such subtle, gradual and hence seemingly chaotic behaviours that show large variances and form noisy patterns are difficult to analyse since they often occur as gradual changes of the activity level or of the intervals between intense activity bouts or of spatial usage patterns. Therefore, disentangling such patterns from the noisy background of stochastic behavioural activity in complex biological systems (Gell-Mann, 2002; Kauffman, 1995) is not trivial, alike, for example, the study of magnetic waves or regional activations and neuronal connections in our brain (Brazier, 1962; Doronina-Amitonova et al., 2015; Ogawa et al., 1990). In the social insects, such more subtle changes in activity or spatial usage may occur during the sensing or processing phase preceding a more specific behavioural action, such as, for example, perceiving a threat that will then lead to a concerted response. Moreover, just like most organisms, also insect colonies show a circadian rhythm (Fujioka et al., 2017; Lei et al., 2021; Siehler et al., 2021), as well as shorter activity cycles (Cole, 1991; Mildner & Roces, 2017; Richardson et al., 2017), which require long-term analyses to be detected. Lastly, long-term analyses are also needed to determine the pace at which colonies go back from an alerted state (like e.g. after entering of an intruder (Scharf et al., 2011)) to their baseline activity levels.

Therefore, despite the fact that many systems have already been developed to automate observations and recordings of insects using computer vision techniques (Balch et al., 2001; Blut et al., 2017; Dankert et al., 2009; Noldus et al., 2002; Sclocco et al., 2020; Shen et al., 2015), many of which focus on individual tracking of tagged individuals, we felt that there is still a need for a data generation and analysis toolkit for collective activity patterns that are inherently noisy and require integration of many data, including many replicates and long durations. We therefore developed ALTAA as a multi-component system for automatized long-term observation, analysis and simulation of individual to colony-level activity in ants, with low computational effort and memory requirements. Our framework contains:

- AntOS: ant observation software and hardware to record the activity of individual or groups of ants,
- Visualizer: visualization software to plot and analyse the collected data and
- AntSim: simulation software to model a theoretical rule-set to compare to the observed data.

Jointly, these three components allow us to detect and describe long-term spatiotemporal patterns in ant behaviour, and to interpret—by comparing the observed to simulated data—which of the patterns are inherent components of individual ant behaviour and which are influenced by the social context, that is, represent emerging collective phenomena. We showcase this in our study by analysing the motion patterns of *Lasius niger* garden ants when either alone, or in groups of six and 10 colony members, respectively. This group size is optimal to capture the transition from individual to collective phenomena, for which a group size below 10 is sufficient (Brahma et al., 2018; Ulrich et al., 2018). While we focused on the emergence of collective actions in our study, our system can easily be expanded—by using larger nest sizes and camera setup accordingly—to larger colonies. Since it allows continuous, high-temporal-resolution monitoring over weeks to months across many replicates, it thus enables studies on short- to long-term activity and rhythmicity of insect groups, as well as spatial usage patterns. Since it does not rely on individual marking, it is robust to birth and death events, and is therefore a valuable tool to analyse colony growth and development from the single queen founding phase to ageing colonies. Because of its low cost and open-source architecture, it can be readily adapted to a wide range of nest geometries and species, and combined with automated perturbations or environmental sensors to investigate how subtle changes propagate through the colony's activity landscape.

2 | METHODS

2.1 | Software and hardware tools for development

All the programmes for this study were developed in Python (version 3.9, retrieved from https://www.python.org) with several packages: OpenCV (version 4.7, retrieved from https://opencv.org), wxPython (version 4.2, retrieved from https://wxpython.org), SciPy (version 1.1, retrieved from https://scipy.org) and Matplotlib (version 3.7, retrieved from https://matplotlib.org).

Arenas for the observation/experiment sessions were designed in Blender (3.0, retrieved from https://www.blender.org) and printed using a stereolithography (SLA) 3D printer (Elegoo Mars 2, ELEGOO, China). The frame for housing the printed arena was made using aluminium beams named as MakerBeam (MakerBeam B.V., Netherlands). A developed software for observation/experimentation were installed and run on a single-board computer (SBC hereafter; Raspberry Pi 4b 4GB RAM, Raspberry Pi Foundation, United Kingdom). A camera (Arducam with Sony IMX477 sensor, Arducam, China) was attached to the SBC for the image acquisition. The camera's maximum resolution is 4056 × 3040 pixels; in this study, we used 2560 × 1440 pixels to reduce image acquisition time. Based on the camera's field of view, the system can capture an area of approximately 30 × 20 cm at maximum. However, to maintain sufficient spatial resolution for ants and reduce blurring or distortion towards the image edges, we limited the observed area to approximately 20 × 15 cm in this study. Although not used in the present experiments, the IMX477 supports infrared illumination, allowing observations of ants under dark conditions.

Approximate costs for obtaining hardware components are listed in Appendix A.

The framework described in this study has three major components: (i) the recording of the behavioural observations during the experiment, accomplished by 'AntOS', (ii) the data analysis conducted by 'Visualizer' and (iii) a possible simulation using 'AntSim', with the latter allowing to run a series of simulations to infer possible rules underlying the observed data (see Figure 1).

Current Python files comprising the aforementioned three programmes, which belong to the group of code named 'cremerGroupApp', are depicted in Appendix B. Some utility functions and classes are used for multiple programmes. Functionalities of two files, 'modFFC' and 'modCV', are used for all programmes; 'modRasp' is used for AntOS, and 'graphFuncs.py' is used for Visualizer and AntSim (see Appendix C).

2.2 | AntOS; apparatus

We protected our experiments from environmental influences by them being performed within a box, built from a frame (MakerBeam) and six wooden panels. The outside of the wooden panels were painted with black matt paint to block outside lighting, while the inside was a bright ivory colour for indirect lighting. To further ensure homogeneous lighting inside the box, the light bulb inside was covered by a light-softening diffuser fabric. The light bulb was a non-flickering LED (12 V, 1.2 W, 120 lumen, 6000 K), which was located at the corner of the apparatus avoiding a direct lighting to the camera lens or the Plexiglas lid of the flat-nest. It also contains a SBC for running AntOS software and acquiring data from a camera (via Camera Serial Interface) and a DS18B20 digital temperature sensor (via General Purpose Input/Output; GPIO pin on SBC); see Figure 2. We designed a 'flat-nest' (Figure 3) providing an arena for the observation, (i) to improve data accuracy by restraining occlusion of individual workers being on top of each other, (ii) to decrease the maintenance and analysis efforts and (iii) to be able to create an arena with complex design. The height of the flat-nest in this study was designed for observation of the black garden ant, *Lasius niger* (Wilson, 1955), considering the worker's body size, approximately 1*mm* wide and 2–3 mm long and a queen body size, approximately 2–3 mm wide and 9 mm long.

After testing multiple heights, we used 1.2 mm of the internal space (Figure 3d) of the arena, and an indentation of additional 2.5 mm (leading to a final height of 3.7 mm) for the queen chamber. This setup restricted the queen to a central chamber, but allowed normal worker activity throughout the nest, yet restraining (but not making it impossible) workers moving on top of one another. At a higher height of 1.5 mm, crawling over each other still occurred regularly, while a lower height of only 1 mm restricted worker activity to certain degree.

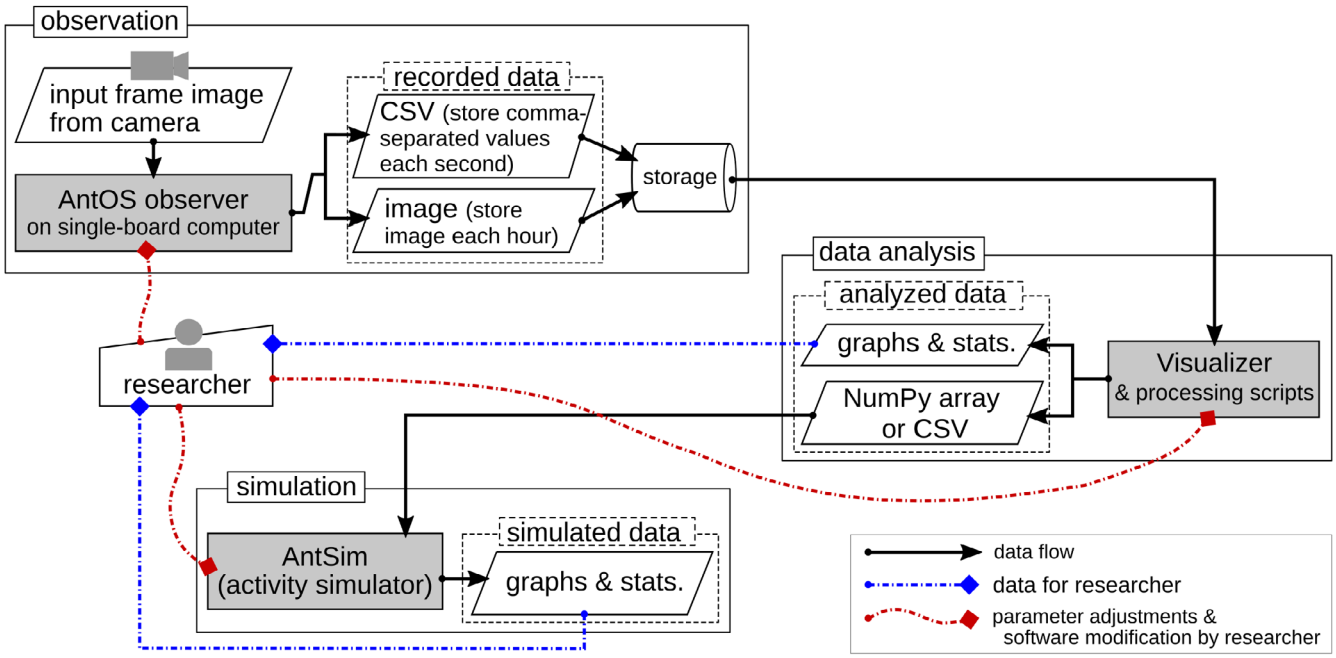

FIGURE 1 Concept diagram of the framework in this work.

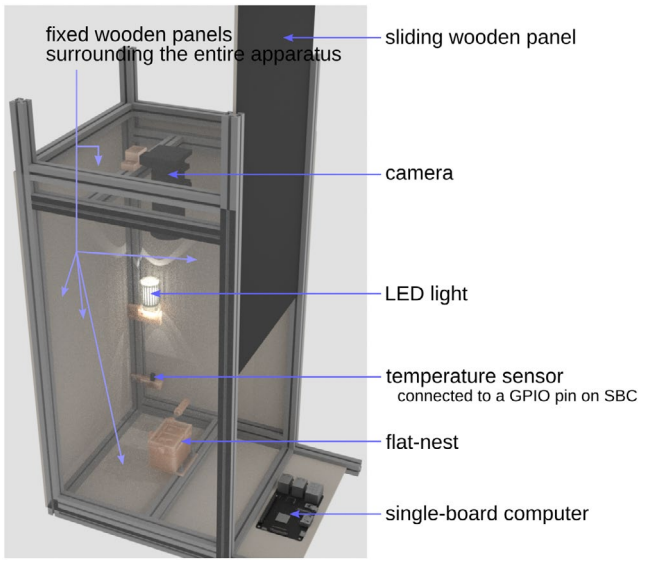

FIGURE 2 AntOS apparatus. *Some of the wooden panels are rendered transparent to display components inside.

The flat-nest can house the ants for observation during a long period such as weeks or months, due to its water container, sucrose container and ventilation holes (Figure 3b-*2* and *3*, and Figure 3c-*5*). The water is provided to the ants through a cotton string in a hole (Figure 3c-*2*), absorbing water from the water container (Figure 3b-*2*). The ventilation holes prevent water condensation on the transparent ceiling, which could otherwise interfere with the image processing. For maintenance of the water and sucrose in the containers (in our case performed on a weekly basis), the AntOS programme is paused while the containers for the sucrose solution and water to be detached and refilled.

Since the flat-nest is produced by 3D printing from resin, the nests have to be carefully post-processed after printing before use to ensure ant health. The toxic effect of the resin material in SLA 3D printing was already reported for zebrafish embryos (Oskui et al., 2016), which could be mitigated by the post-processing using ultraviolet (UV) light.

To prevent toxic effects for the ants, which can show as reduced movement or activity, cessation of queen egg laying and even death, the newly printed flat-nest should be (1) cleaned using isopropyl alcohol (IPA), (2) exposed to UV light, (3) water-washed and dried in a well-ventilated space and (4) tested with a small number of workers. If any abnormal behaviour is noticed, the above steps should be repeated. The length of the IPA cleaning and UV light exposure varies depending on the resin type and its production company. The FDM (Fused Deposition Modeling; filament type) 3D printing could be used with less safety steps, yet it has a reduced printing resolution compared to the SLA.

Moving a colony or multiple workers of *L. niger* into the flat-nest could be difficult due to the low height of the arena. We propose to first add the queen and brood into the open nest and then to move workers into the closed arena using a funnel and a tube (see Figure 4). For this procedure, a transparent rubber tube is prepared with one side blocked with a cotton ball and another side with a funnel attached, which is also 3D-printed with the matching diameter to the tube. To prevent the ants from climbing out of the funnel, polytetrafluorethylen (PTFE, like Fluon) can be applied to its interior walls. To first trap the ants in the tube, they can be dropped into the funnel using tweezers; then, the funnel is tapped to make them fall into the tube. Then, the upper end of the tube is blocked by another cotton ball. After removal of the funnel and the first cotton ball, the tube is quickly connected to the arena. The ants in the tube are encouraged to move into the arena by softly pushing

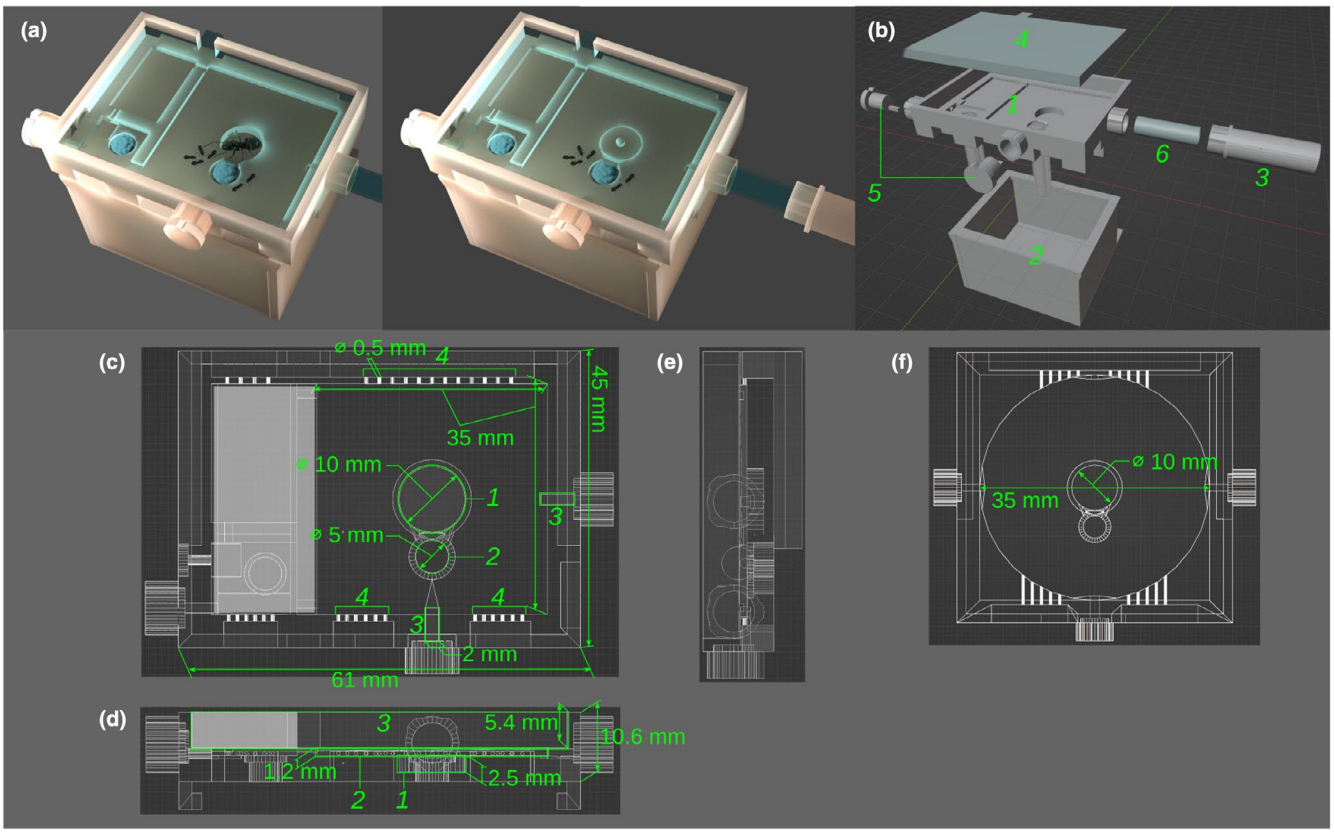

FIGURE 3 Flat-nest; (a) overview of the flat-nest with and without a queen ant, (b) major parts; *1*: arena, *2*: water container, *3*: sucrose solution container, *4*: transparent Plexiglas lid, *5*: plugs for outward passages, *6*: transparent rubber tube (mm), (c) top view of a square-shape arena. A secondary chamber (greyed area on the left side) was not used in the current study; *1*: circular indentation when housing a queen ant, *2*: hole for cotton string to provide water, *3*: outward passages, *4*: ventilation holes, (d) Front view of the arena; *1*: deeper area for a queen, *2*: shallow area for workers, *3*: place for transparent lid, (e) side view of the arena, (f) top view of the second flat-nest with circular-shape arena, used in the current study.

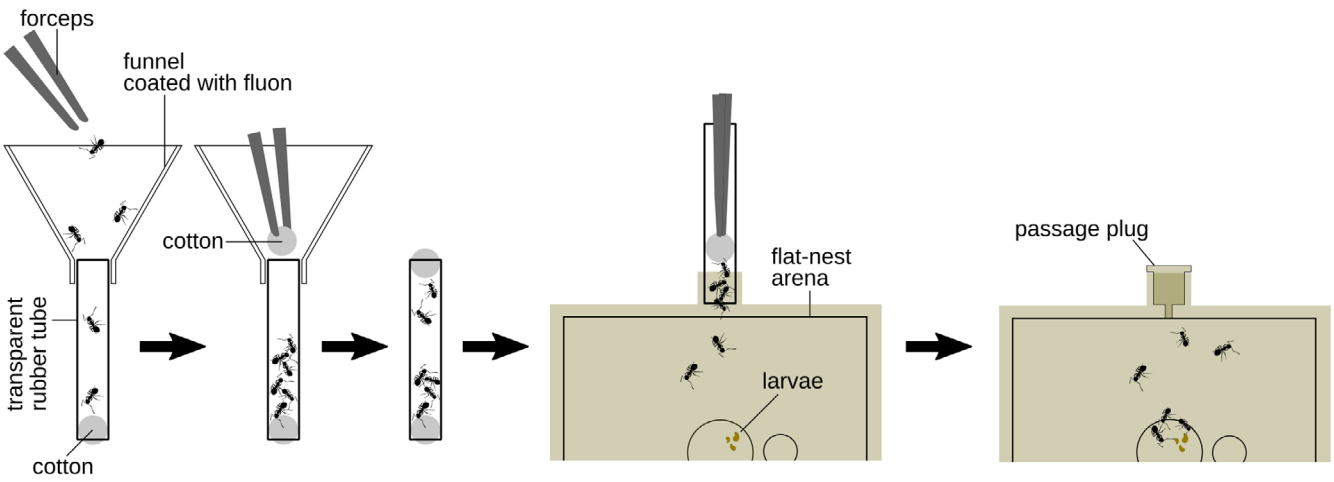

FIGURE 4 Introducing ant workers into the flat-nest arena.

the remaining cotton ball. We found workers to typically quickly move to and stay in the arena, also being attracted by the wider space and the brood items in the arena. After ant integration, the passage can be either blocked with a printed plug or connected to another section such as a sucrose container or a chamber.

2.3 | AntOS; software

The AntOS programme collects data from the camera and other sensors in apparatus, like the temperature sensor. In the graphical-user-interface (GUI) of AntOS, the user can adjust several options

including the camera index used, the session duration, the regions of interest (ROI), intervals for the temperature logging and saving ROI images to files, colour values in HSV colour space (Hue, Saturation and Value) for detecting the inherent ant colour or an applied colour marker. The number of ROIs, which can be set in the frame image, depends on the size of the flat-nest and the camera type. In the current study, we set ROIs to three. Upon starting it, the programme (i) reads and processes a frame image from the camera every second to save resultant data in a CSV data file for each ROI, (ii) records the temperature inside the AntOS apparatus every 10 min (adjustable) to a log file and (iii) saves an image of each ROI as a JPEG image file every hour (adjustable). The image files and the resultant CSV data files for each ROI are saved in a separate folder.

Frame processing is used to detect motion to store centre points of motion segments, detect ant colours to store its rect (rectangle denoted by *x*, *y*, width and height) info and a possible additional colour code applied to the ants (not performed in the current study) to store its position. For the motion detection, AntOS calculates the difference in consecutive frame images, finds contours from the difference between images, calculates the centre point of each contour and saves the *x*/*y* coordinates of contours with a timestamp in the resultant CSV file. For the ants' colour detection, it detects blobs with the user-defined HSV colour and stores the rect of each blob's contour, yet AntOS can be used without this additional information only based on motion data, as in the experimental study described below.

The temporal resolution of the frame processing is set to 1 s due to the time needed for frame retrieval of the SBC from the camera and running the processing Python code. AntOS on the currently used SBC takes 0.5–0.6 s to retrieve the frame image (1920 × 1440 resolution) and an additional short time (depending on the number of blobs that moved in each frame) to run the image processing code. The part (ROI) of the frame image is saved as an image file every hour to allow the experimenter to check for possible artefacts or disturbances to the system, such as a software error or physical disturbance of the apparatus during the session, which would affect the resultant data. The filename of each saved image is a timestamp. By following use of the Visualizer programme (described below), motion centre points, occurred at certain times, can be drawn on the ROI image that was saved at that exact time. It draws all the corresponding motion points to all the saved images at each hour so that the user can check each motion point is drawn on the ants in the images.

The AntOS code is split into three files, considering the code modularity, 'antOS.py' for the GUI, 'modSessionMngr.py' for calling functions on the scheduled time during the session and 'modRasp.py' to retrieve the frame image and send/receive data to/from sensors/actuators via GPIO pins on the SBC. For different functionalities depending on the experimental setup, the image processing can be modified in 'modSessionMngr.py', and managing sensors and actuators attached to GPIO pins can be modified in 'modRasp.py'.

2.4 | Data exploration/visualization; visualizer

The Visualizer programme is to draw graphs and images (such as heatmap images or screenshots) from the data obtained by AntOS. These observed data from the experiment can later be compared to theoretical rules of ant behaviour by producing processed data sets in a NumPy (Harris et al., 2020) array for the simulation software AntSim, detailed below. The main functions of the Visualizer programme lie in the analysis of motion-point data, as showcased in our experimental study below. After selecting a data folder, the user can select a graph/image type to draw, set different parameters and press the 'draw' button in the GUI to start bundling data with a user-defined interval (such as several seconds or minutes to be represented as a single data point in the resultant graph) and drawing a graph with the bundled data. It offers the following options to draw different graphs or images:

- *initImg* shows the first image of all saved ROI images. This is for setting parameters directly from the image. On the loaded image, the user can mouse-click/drag to select certain points such as a brood/food/garbage position, the region of interest and an area of grid cells.
- *sanityChk* is for the user to check if motion points occur only on the ant's body with the saved ROI images to detect possible artefacts.
- *intensity* draws a graph with the number of motions in each bundled data point.
- *intensityL* draws a graph of the number of motions around three user-defined locations: brood, food and garbage.
- *dist2b* draws a graph with measurements of the maximum (among all motion points in the data frame) distance between the brood position and a motion point in the bundled data.
- *intensityPSD* draws the power spectral density graph using Welch's method (Welch, 1967) on the data processed with '*intensity*'.
- *spAHeatmap* draws a heatmap image with the motion points.
- *spAGridHeatMax* & *spAGridHeatMean* draws a graph with the max/mean value in each grid-cell of the heatmap during a given time (bundle interval).
- *proxMCluster* draws a graph with the motion cluster value, which represents multiple ants moving next to each other for a certain duration (≥3 s). It is described with a pseudo-code in Appendix D.

2.5 | Simulation; AntSim

With AntSim, the user can simulate motion data following theoretical rules of ant behaviour, based on any a priori hypotheses of ant decision rules or inferred from the real-world experiment in Visualizer (such as differences in activity patterns between group sizes, colonies). In our example, we use the data of individual ants to infer the activity patterns of groups in case the ants would not affect each other's behaviour. By comparing these theoretical patterns to the observed patterns in grouped ants, we can infer how

the presence of nestmates influences, for example, inactivity duration and temporal activity patterns of the ants. This is possible since AntSim simulates motion data in the same temporal resolution and format as the raw real-world ant data acquired by AntOS. The resultant graphs from the simulated data can be directly compared to the output of Visualizer using the real-ant data to highlight deviations between observed and theoretically expected to evaluate the validity of the theoretical underlying rules for ant behaviour. The main focus of the current AntSim is to simulate temporal activity patterns of ant groups, following the simulation procedure outlined in Figure 5 with a set of user-defined parameters: length of data, data-bundle interval, interaction of workers and threshold ranges to boost the distribution of the activity and inactivity durations.

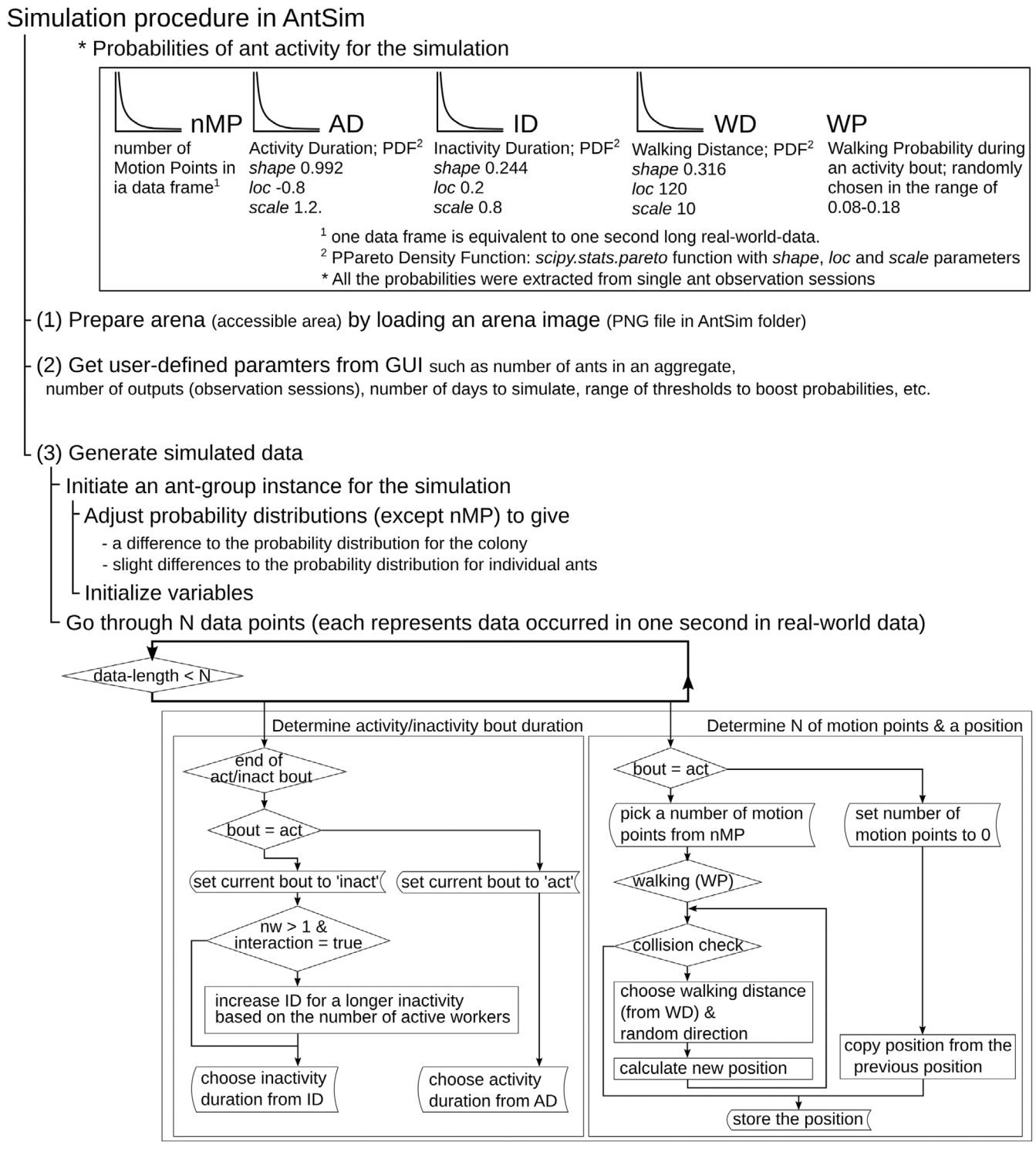

FIGURE 5 Simulation procedure in AntSim.

We have implemented two major simulation types (i) '*n[N]_[i or s]*; where *N* is the number of ants, *i* is for interaction among ants and *s* is for non-interactive ants', and (ii) '*mComp_[i or s]*'. When the simulation procedure is finished, the programme outputs an intensity barplot, its power spectral density, boxplots of the activity and inactivity durations, and heatmap images. In '*mComp_[i or s]*', ant groups with the same parameters, but of different group sizes (one, six and ten), are simulated. With this simulation option, intensity barplots, power spectral density graphs, boxplots of the activity and inactivity durations, and heatmap images are produced for each group size. Additionally, a comparison graph for the number of movements by group size is produced.

2.6 | Experimental study

We were here interested in analysing the spatial and temporal activity patterns of *L. niger* workers when alone or in a group of six and ten ants, in the presence or absence of brood and in different nest architectures. To this end, eleven colonies of this monogynous and monomorphic species common to the Northern hemisphere, were reared from queens collected during a large nuptial flight (which regularly occur from July to August, Czechowski et al., 2012; Wilson, 1955) in Klosterneuburg, Austria in July 2022. Collection of this unprotected ant species was performed in compliance with international regulations, in particular the Convention on Biological Diversity and the Nagoya Protocol on Access and Benefit Sharing (ABS), and all experimental work followed European and Austrian law and institutional ethical guidelines. After collection from the field, the queens were reared in the dark to a fully grown colony with workers in plastic boxes (Tupperware) containing a constant supply of water, 1*M* sucrose solution and dried mealworm powder. Routine maintenance work, including providing water and food and cleaning, was performed every week.

We analysed two experimental setups:

1. To test for the effect of group size on activity, one, six and ten worker ants per colony were sampled randomly (except for avoiding freshly emerged callow ants) and housed in one flat-nest each of the square arena type (n1, n6 and n10; Figure 3c). Several mid- to late-stage larvae from the same colony had been added per replicate. The motions of the three group sizes per colony ($n=11$) were recorded for 1 week each between September and November in 2022.
2. To test for the effect of brood presence and nest architecture, we repeated the experiment 1 year later (from July to October in 2023) for the sizes of one and six workers (n1* and n6*), to compare these new setups without larvae and being placed in a round instead of square arena to the previous n1 and n6 replicates (see Figure 3f).

We collected data by AntOS, analysed it by Visualizer and simulated temporal activity (Figure 5) by AntSim. Statistical comparisons (Wilcoxon signed rank and rank sum tests, Kruskal–Wallis tests) were performed in R (version 4.1.2). In pairwise post hoc comparisons and due to reuse of the n1 and n6 data with larva for their comparison to the n1* and n6* larvae-free situation, Bonferroni corrections were used to adjust for multiple testing. Two-sided, adjusted *p*-values are reported.

3 | RESULTS

3.1 | Intensity; number of motion points

We first analysed activity 'intensity' denoted by the number of motion points in a given duration, with example graphs being shown in Figure 6a. When comparing the intensities between the group sizes of six versus ten ants, the n10 motion was lower than expected by sheer upscaling from the six ants group size ($m / 6 \cdot 10$, where m was the number of motions of n6 from the same colony; median 0.896 instead of the expectation of 1.0; Wilcoxon rank sum exact test, two-tailed test, $W=22$, $p=0.01$). This indicates that increasing the group size from six to ten ants did not lead to a proportional increase in motion. Because the available space per ant remained nearly unchanged in this setup (arena area: $\approx 1146\,mm^2$; free space $\approx 1128\,mm^2$ for six ants vs. $\approx 1116\,mm^2$ for ten ants), reduced motion is unlikely to be explained by a simple reduction of individual occupation space. Occasional collisions or brief pauses during close encounters may also contribute to the lower total motion at larger group sizes. Overall, these results suggest a deviation from linear scaling of individual activity. Note that we derived the expected value for the 10 ants only from the six ants and not from single ants, as the latter may show substantial individual differences. When comparing same-sized groups with and without larvae being present, we could not detect any significant differences in the sum of intensity (Wilcoxon signed rank exact test; n1 vs. n1*: $V=51$, $p=0.123$, n6 vs. n6*: $V=48$, $p=0.206$).

3.2 | Temporal pattern

To describe the temporal activity pattern or periodicity of the ants, we calculated the power spectral density for the different group sizes (n1, n6 and n10) per colony. In contrast to *Leptothorax* ants (*L. allardycei*, Cole, 1991; and *L. acervorum*, Boi et al., 1999; Richardson et al., 2017) that show activity peaks every 15–30 min, we found no synchronized short-term activity peak in *L. niger* ants in our experiment. Yet, many unconcerted peaks of activity occurred within the period of 20–120 min. The mean power in this long duration range of 20–120 min. was approx. double than that in the short duration range of 10–20 min (Figure 6).

The resulting fractions of ~2.0 were consistent across group sizes (Kruskal–Wallis rank sum test; chi-squared = 0.076, df = 2, $p=0.963$). However, the fraction dropped when there were no larvae, reflecting that the presence of larvae stimulates the

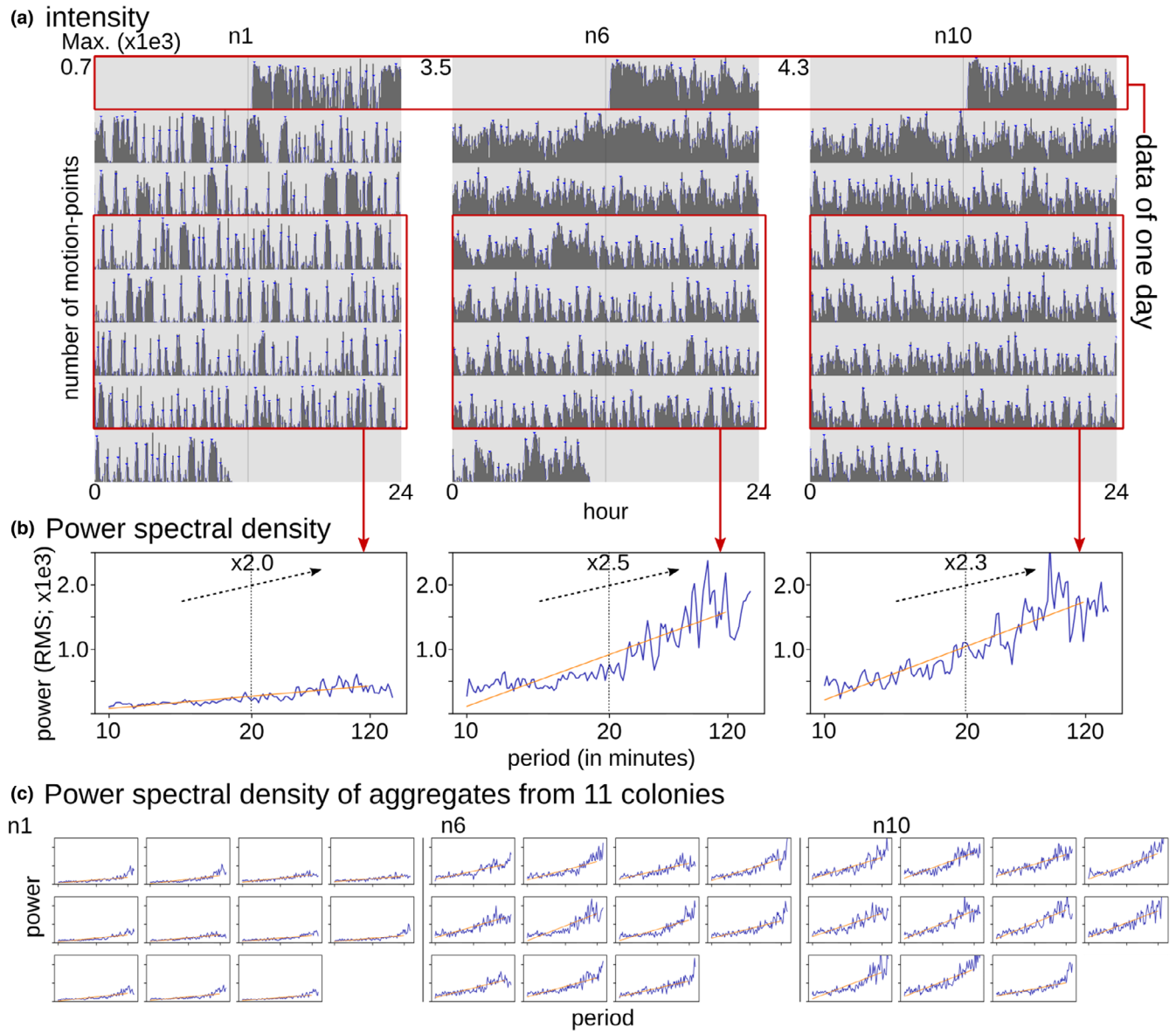

FIGURE 6 (a) Activity intensity (number of motion points); n1, n6 and n10, as exemplified from one colony, (b) power spectral density graphs of the intensity data shown in a (from 4 days in the middle of the session). The values on the *y*-axis are root-mean-square values and the float number in the middle of each graph indicates the fraction of mean power values of longer to shorter period. (c) Power spectral densities of n1, n6 and n10 for all 11 colonies.

worker ants' activity to be more periodic in the long duration of 20–120 min (Figure 7, Wilcoxon signed rank exact test; n1 vs. n1*: $V = 66$, $p < 0.001$, n6 vs. n6*: $V = 60$, $p = 0.014$). Note that this fraction drop occurred despite the fact that overall activity intensities did not differ in the presence or absence of larvae (see Section 3.1).

3.3 | Spatial pattern

To analyse the ants' spatial usage preferences, we used Visualizer to create heatmaps and graphs (Figure 8). By comparing same-sized groups with and without larvae respectively, we found that workers are strongly attracted to larvae by showing higher activity in the centre area in the presence of larvae (Figure 8a,b), and performing a more localized activity with larvae (Figure 8c). Figure 8b shows that the attraction point of groups with larvae (n1, n6 and n10) was all quite close to the centre, while groups without larvae (n1* and n6*) rather stayed away from the centre.

Also, the ants are attracted to edges or wall-like structures, as groups of all sizes show high activity around the edges of the arena (Figure 8a). Figure 8d shows that ants walk along the edges, that is they have a higher probability of walking to the perpendicular directions in the square arena compared to the circular arena (Figure 8d). Moreover, they seem to be attracted to the water source (high activity of n1* and n6* around the water source; Figure 8a).

The interquartile ranges (IQR) of the probability distributions of n1, n6 and n10 (Figure 8c) reveal that activities are more dispersed in groups of 6 or 10 ants compared to single ants (Kruskal–Wallis

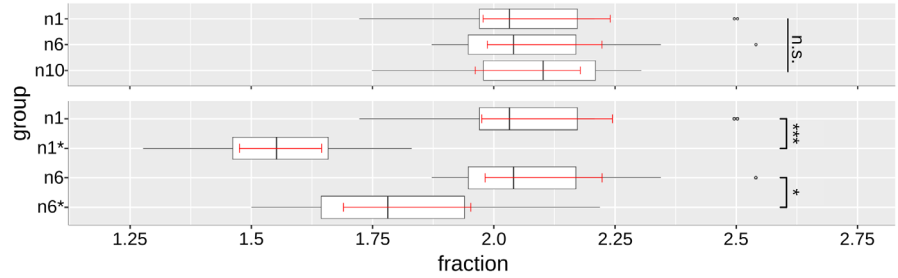

FIGURE 7 Fractions of mean power in the long duration range over the short duration range (upper figure) for the three group sizes with larvae (n1, n6 and n10), and (lower figure) for same-sized groups with and without larvae (n1 vs. n1*, n6 vs. n6*). Boxplots show the median and interquartile range (IQR). Whiskers extend to the most extreme data points within 1.5 × *IQR* of the quartiles; points beyond this range are plotted as outliers (dots). Red error bars indicate the 95% bootstrap confidence interval of the mean. Significant differences between contrasts are depicted as * for $p < 0.05$, ** for $p < 0.01$, *** for $p < 0.001$, and n.s. for non-significant. Data from all 11 colonies.

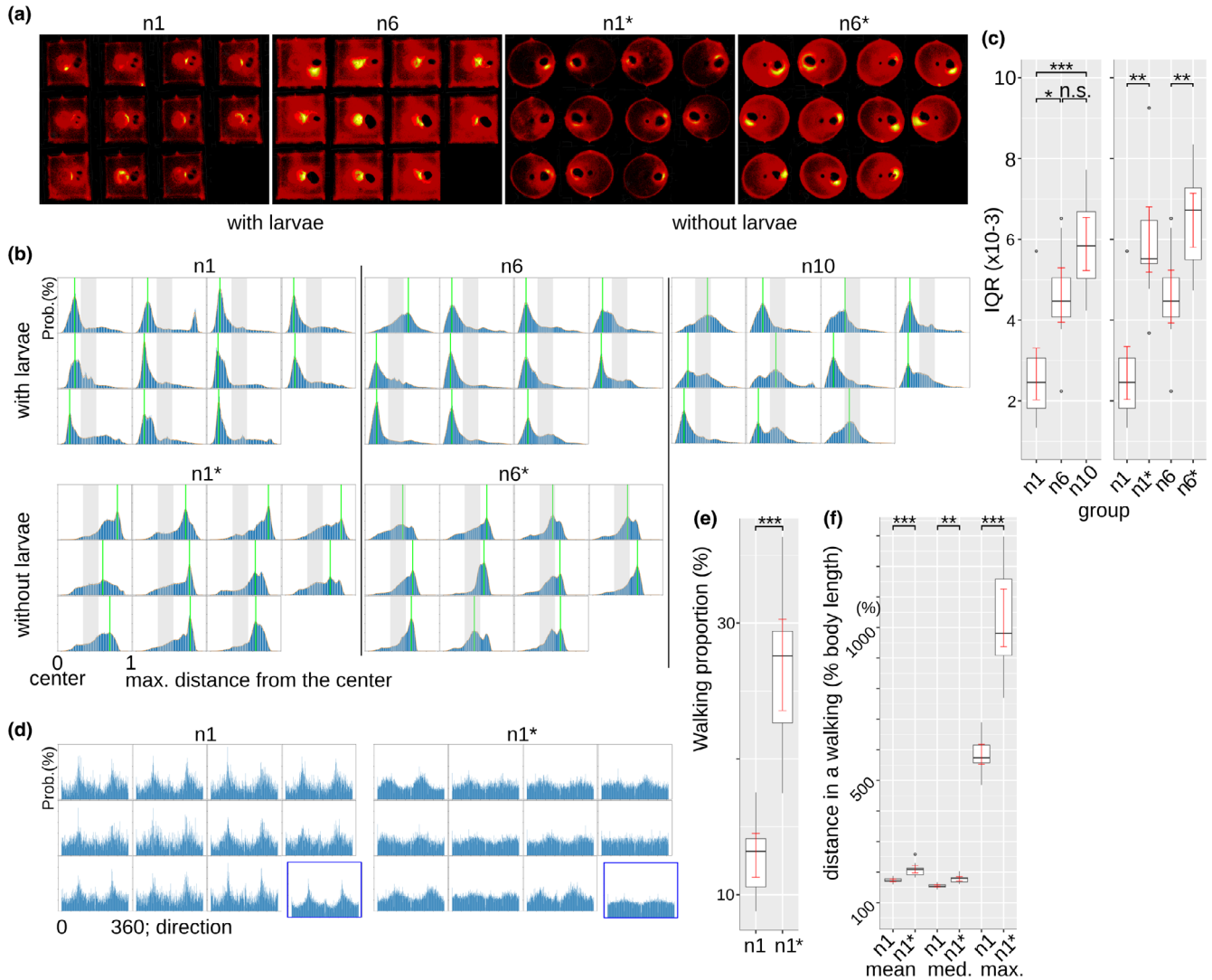

FIGURE 8 Patterns of ant spatial usage shown as (a) heatmap of motion points in single ants or groups of 6 ants, both with and without larvae and in the square versus circular arena (yellow indicates higher activity than red, black indicates no activity), (b) distributions of the distance (from the arena centre) of each colony in n1, n6, n10, n1* and n6* (grey zone depicts the distance to the water cotton ball and the green line depicts the highest peak distance), (c) interquartile range of analysis (b), with single ants and groups or 6 compared both by size and presence/absence of larvae, (d) direction (in degrees, with 0 pointing right and angles increasing counter clockwise) probability of single ants when walking in the square versus circular arena (distance of two motion points in two consecutive frames exceeding 120% of the ant's body length). The last graph marked with blue rectangle for each group size displays the mean probability distribution, (e) the percentage of walking in single ants and (f) a comparison of the single ants' walking distance (in terms of ant's body length) with and without larvae. * Boxplots are formatted as in Figure 7.

rank sum test; chi-squared = 18.131, df = 2, $p < 0.001$; pairwise Dunn's test for post hoc comparisons with Bonferroni correction: n1 vs. n6, $p = 0.036$, n1 vs. n10 $p < 0.001$, while n6 vs. n10, $p = 0.256$). Comparison of the IQRs of single ants resp. groups of 6 ants with and without larvae, revealed that the ants showed more dispersed activity when without larvae, which was true for both single n1* and grouped n6* ants (Wilcoxon signed rank exact test; n1 vs. n1*: $V = 2$, p-value = 0.003, n6 vs. n6*: $V = 5$, p-value = 0.01, Figure 8c). For single ants, we also found that its walking percentage was significantly higher when the ant was without larvae (and in a circular arena) than when it was with larvae (and in a square-shape arena). See (Figure 8e), Wilcoxon signed rank exact test; n1 vs. n1*: $V = 0$, $p < 0.001$. Here, walking was defined by the following criterion; the distance of two motion points in two consecutive frames (in 1 s) exceeded 120% of ant's body length. Also, single ants without larvae walked longer distances (Figure 8f, Wilcox signed rank exact test; n1-mean vs. n1*-mean: $V = 0$, $p < 0.001$, n1-Median vs. n1*-Median: $V = 1$, $p = 0.002$, n1-Max. vs. n1*-Max.: $V = 0$, $p < 0.001$).

3.4 | Response of groups to disturbance

By transferring the ants from their stock colony to the experimental filming arena, the ants experienced a sudden change in conditions. We therefore used our system to analyse whether their activity was different in the first period after the disturbance and after which time activity levels would indicate an acclimation to the altered condition. We analysed the temporal decrease in activity following disturbance by subtracting each colony group's median value and then normalizing the resulting values by the maximum value. The time series was then smoothed using a moving average over 13 bins (±30 min). We fitted an exponential decay model

$$A(t) = A_0 e^{-kt},$$

where A_0 represents the initial activation amplitude and k the decay rate. The decay half-life was computed as

$$t_{1/2} = \frac{\ln(2)}{k}.$$

These model fits are shown in Figure 9a, where the red curve indicates the fitted exponential and the number above each panel reports the estimated $t_{1/2}$ in hours. All fitted values for A_0, k and half-life for each colony are provided in Appendix E. We found that the ants, when in groups of 6 or 10, but not when alone, showed an initial high activity level, which then gradually subsided within 2–3 days. Groups of n6 and n10 exhibited an initial activation followed by a gradual decrease in activity over 2–3 days. In contrast, n1, n1* and n6* did not show a distinct activation increase and consequently displayed inconsistent decay dynamics. Variance-based comparisons of half-life values revealed significantly higher variability in n1, n1* and n6* compared to n6 and n10 (Bartlett pairwise tests, $p < 0.001$), indicating the absence of a structured activation–recovery process in those groups (Figure 9b). Half-life values of n6 and n10 did not differ ($p = 0.57$). The activation amplitude A_0 clearly separated the groups: n6 and n10 had significantly higher values than n1, n1* and n6* (pairwise Wilcoxon rank sum tests with Benjamini–Hochberg correction: all comparisons $p < 0.05$; n6 vs. n6*, $p = 1.4 \times 10^{-5}$; see Figure 9c). No difference was detected between n6 and n10 ($p = 0.61$).

We further used 'proxMCluster' to analyse the bundled-up behaviour, measuring the activity intensity produced by multiple ants that are in close proximity (see Algorithm 1 in Appendix D). Many ant groups showed distinctively high values at the very beginning, followed by smaller peaks throughout the week (Figure 10a). However, when larvae were absent, the ants' overall activity when close to each other was significantly lower (Figure 10c) and the otherwise observed distinctive high value at the very beginning was mostly absent (Figure 10b). This significant lower activity within the proximate range to nestmates was observed while the overall activity was not significantly different (see Section 3.1).

3.5 | Simulation results

In our study, we used AntSim to first simulate the activity of individual ants and then examine insofar these rules at the individual level could reproduce group-level patterns observed in our empirical data by simple upscaling. Specifically, we aimed to capture two key features: (1) temporal fluctuations in activity (3.2) and (2) reduced overall activity levels in the n10 group (3.1). Since we found that scaling up of average individual behaviour was unable to appropriately capture real-word collective behaviour, we applied additional simulation steps by added rules that helped us to retrieve the collective behaviour. Therefore, in our work, we used the simulation to construct a bottom-up model of ant colony dynamics by implementing simple behavioural rules over time. AntSim can be used in this way, yet also implementing more theoretical rules from a priori hypotheses to evaluate their relevance for understanding complex collective behaviours.

To ensure that our simulations reflected steady-state behaviour rather than the initial transitional effect, we restricted the simulation result comparison to a 96-h period following an initial 60-h acclimation phase, based on observations of real ants adjusting to the flat-nest environment. We began by extracting activity and inactivity duration distributions from single-ant data (n1, $n = 11$), computing the average probability distribution across individuals. The simulations based solely on these average distributions failed to reproduce the patterns observed in real data.

This discrepancy arose because averaging across individuals led to an underrepresentation of longer activity and inactivity durations, which are essential for capturing the variability and stochasticity observed in real ants. To address this, we applied a probabilistic 'boosting' to the tail of the duration distributions for each simulated ant. Specifically, for each individual, we selected a threshold duration by adding a small random deviation to a group-level reference value, which was itself randomly chosen within a predefined range (0 – 300 s for activity, 600 – 1200 s for inactivity, based on empirical

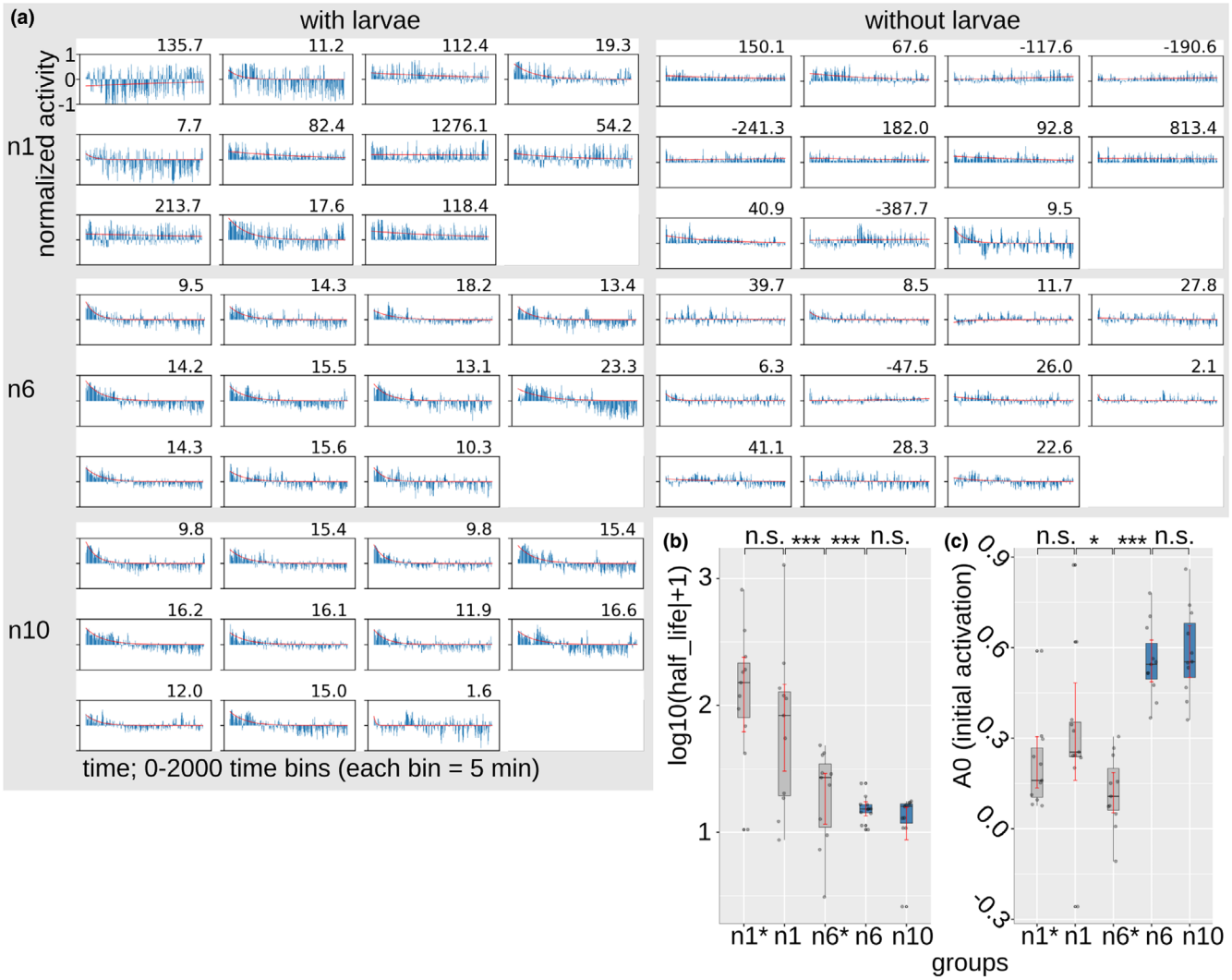

FIGURE 9 (a) Activity fluctuation for one week in single and grouped ants and in dependence of larval presence/absence. Zero on the *y*-axis represents the median of activity. Each vertical bar represents the smoothed 5-min activity data. The red line shows the fitted exponential decay curve, and the number above each panel indicates the estimated half-life of the decay. (b and c) Distribution of (b) log-transformed half-life and (c) A_0 values across groups. Grey dots show individual colonies, boxplots show group distributions. Boxplots are formatted as in Figure 7.

observations). We then increased the probability mass of durations exceeding this threshold by applying a multiplicative scaling factor, iteratively adjusted until the total tail probability reached at least 0.05. This adjustment allowed the simulations to retain the overall statistical structure of the group-level data while introducing individual variability necessary to reproduce the long-tailed distributions observed in real ants. Adding this boosting step improved the fit between simulated and real ants' activity patterns (Figure 11a). Statistical comparison using the Wilcoxon rank sum test showed that simulation without boosting (sim.1) differed significantly from real data ($W=23$, $p<0.001$), while simulations with boosting but no interaction (sim.2) showed no significant difference ($W=432$, $p=0.152$).

However, sim.2 still failed to replicate the reduced activity levels observed in n10. To address this, we introduced an interaction rule: When many ants in the group were active simultaneously, the probability of longer inactivity durations increased for each individual. This rule was motivated by the hypothesis that ants may reduce their own activity when others are already active, possibly reflecting redundancy or energy conservation mechanisms. With this addition (sim.3: boosting + interaction), the simulation reproduced both the activity fluctuation pattern and the reduced activity intensity in the n10 group. The Wilcoxon rank sum tests showed no significant differences between real data and sim.3 for both overall activity fluctuation ($W=454$, $p=0.25$) and n10 inactivity patterns (Figure 11b; $W=83$, $p=0.151$).

In summary, our simulation approach was built bottom-up, starting from simplified individual-level rules and progressively incorporating minimum essential features to reproduce the collective behaviour patterns observed in real ants.

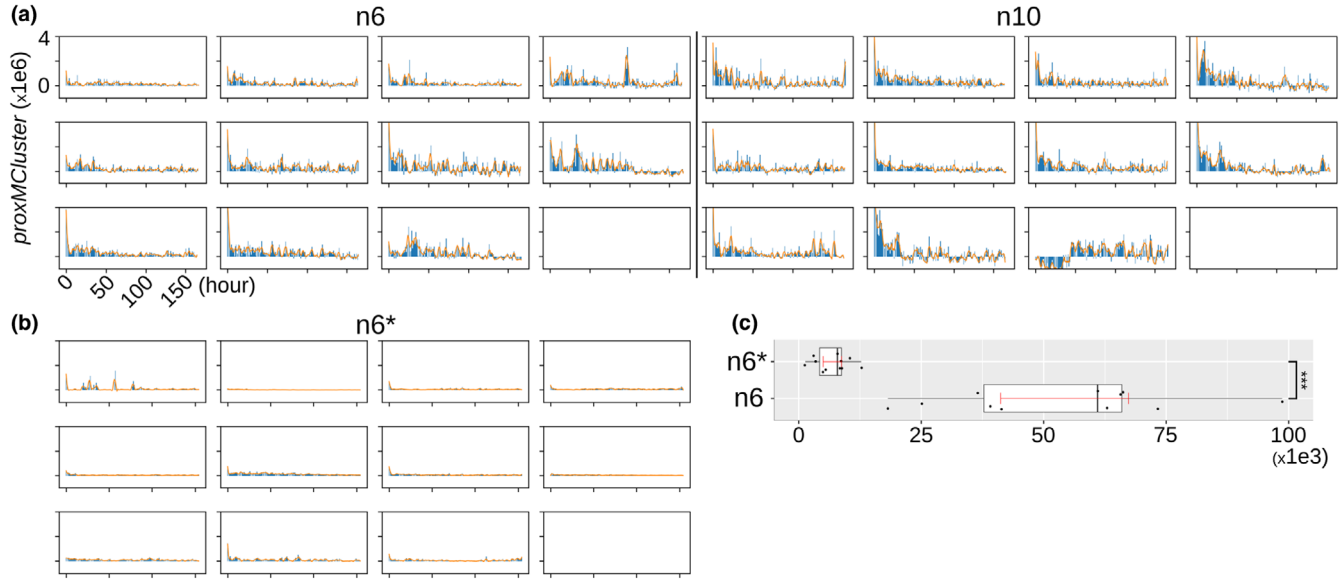

FIGURE 10 Bundled activity intensity. Graphs of 'proxMCluster' with zero on the *y*-axis representing the median. An individual vertical line shows the data for 1 h. (a) Graphs of groups of 6 and 10 ants with larvae. (b) Graph of the group of 6 ants without larvae. (c) Comparison of mean values of n6 and n6* (Wilcoxon signed rank exact test; $V = 66$, $p < 0.001$). * Boxplots are formatted as in Figure 7.

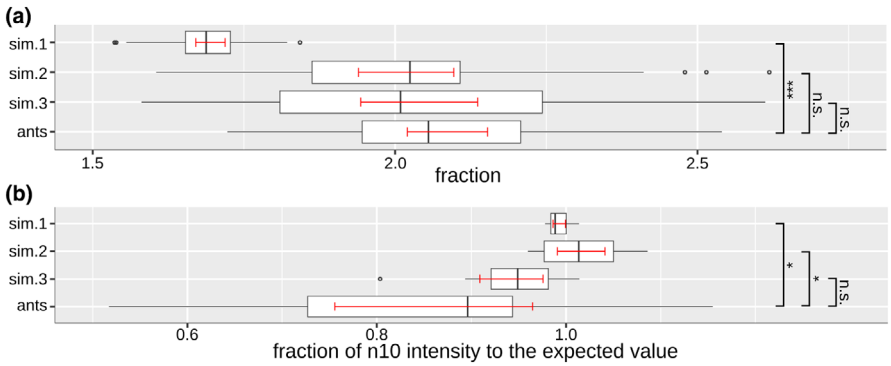

FIGURE 11 Comparison of simulated data to the real-world data; sim.1: No boosting and No interaction, sim.2: Boosting and No interaction, sim.3: Boosting and Interaction, ants: Real-world data. (a) Comparison of fractions in the longer to the shorter period range. (b) Comparison of fractions of n10 activity to the expected value by linear increase from n6. * Boxplots are formatted as in Figure 7.

4 | DISCUSSION

We have developed a multicomponent system that can be utilized for studying long-term behavioural changes of groups of ants or other insects. It is a collection of tools, consisting of (i) a custom-designed nest preventing occlusion during data acquisition, (ii) a recording system running on a single-board-computer and (iii) several programmes in Python for data acquisition, analysis and simulation. All software and design (Blender) files of the flat-nest are available via the Github repository, https://github.com/jinook0707/cremerGroupApp. AntOS, Visualizer and AntSim are located in 'antOS', 'visualizer' and 'antSim' subfolders, respectively. The design files are located in 'blenderFiles' folder.

We here showcase the use of our system by an experimental study comparing the activity of *L. niger* worker ants differing in group size (1, 6, 10 ants), presence/absence of larvae and nest architecture (square vs. circular). The collected data are available in https://zenodo.org/records/16893940. The use of AntOS allowed us to derive the following behavioural characteristics from our experiment:

1. The activity intensity (amount of motions) in ant groups was found to be lower than the expected value of the linear increase with the number of workers. This finding is consistent with previous studies on ants, such as *Camponotus rufipes* and *Temnothorax rugatulus*, which reported sublinear scaling of locomotor activity and energy expenditure with group size (Ferral et al., 2018; Napoli et al., 2025).
2. A weak periodicity in the lower frequency range (longer duration range; 20–120 min) was observed independent of group size. Because this weak periodicity did not show a particular peak on a specific duration, we used a fraction of the long duration range to the short duration range, which was 2.032, 2.041 and 2.102 (median values) in n1, n6 and n10, respectively. In the absence of larvae (in a circular arena), the periodicity became even weaker and the fraction dropped to 1.552 and 1.781 for both single (n1*) and groups of 6 ants (n6*). This suggests that a weak periodicity occurs

in *L. niger* workers, which is promoted further by presence of larvae or nestmates, with the latter having a less strong effect than brood presence. Our data thus add to distinct findings on the effect of brood on ant activity cycles. Whereas brood presence can increase the degree of periodicity in some species (Cole & Trampus, 1999), work on *Diacamma* ants describes that brood care can also lead to a suppression of a circadian (24 h) rhythmicity, inducing around-the-clock activity of (Fujioka et al., 2017). These differences between studies may reflect both biological differences and differences in experimental conditions, such as light conditions or other environmental conditions that may affect periodicity.

3. Workers are spatially attracted to larvae, edges (or walls), the water source and nestmates, which is consistent with previous findings in other ants (*Leptothorax unifasciatus*; Sendova-Franks & Franks, 1995) or in the same species as used in this study (*L. niger*; Depickère et al., 2004).
4. Single *L. niger* workers with and without larvae showed similar activity levels (total amount of motions). Yet, in the presence of larvae, the ant seems to spend more time for non-walking behaviours such as grooming and care-taking. In the absence of larvae, it spends more time walking, similar to the report from other ant species (Koto et al., 2023) in which isolated ants without any other individuals moved longer distances.
5. Groups of *L. niger* workers, but not individual ants displayed higher activity in the beginning of the experiment, and decreased their activity levels over 2–3 days to reach a stable activity level after acclimation to the experimental condition, consistent with findings in *Temnothorax* ants (Popp & Dornhaus, 2023). Notably, this increased initial activity was dependent on larval presence. This larva–worker interaction is consistent with previous findings (Cole & Trampus, 1999; Dunn et al., 2024). Although the number of workers in the group might affect the initial high activity to a certain degree, it was statistically not significant. Larval presence also triggered higher activity of workers in close proximity to their nestmates. This suggests that ant groups with larvae in a new environment first highly increase their activity, keeping short distances to other nestmates, then gradually increasing the distance between nestmates, likely for exploration of the new space, and gradually decreasing the activity level to a stable state.

We further used AntSim to evaluate our real-world observations by comparing them to simulated data. For our purpose, we derived individual activity rules from our single ant case and by inferring them from the n1 data obtained by Visualizer. After implementing the rules in AntSim for ant group scenarios, we could verify that collective activity patterns are 'not just many individual ants'. Instead, our approach helped us to infer, which additional simulation rules are required to produce results that match the observed experimental data for grouped ants, allowing for further interpretation of the underlying biological rules for collective behaviour. Currently, AntSim only produces reliable data for temporal but not yet spatial activity patterns, which will require further experiments and methodological developments.

Our system can be extended by adding more sensors and actuators to the SBC to enable different types of automated data collection and experimental manipulation such as, for example automated increase/decrease of temperature and humidity.

The testing groups comprising only 1, 6 or 10 individuals in our experiment are insufficient to represent colony-level activity. This study was intended as a proof-of-concept to demonstrate the basic functionality of the system rather than to capture collective behaviours at the colony scale. Nevertheless, scaling up to experiments with 100 or more individuals could be readily achieved by increasing the flat-nest diameter to approximately 10 cm or larger. Since ants are highly social species, they regularly cluster together, so that—as in our comparison of 6 and 10 ants above, a full colony size is not expected to exorbitantly increase collisions of colony members. When working with larger ant species, additional modifications to components such as the flat-nest, supporting frame and camera calibration would be required. However, a fundamental limitation of the current system is that it does not permit three-dimensional nest structures or structural modifications by the ants themselves, which are essential aspects of natural nest-building behaviour. (Leckie et al., 2025; Leclerc et al., 2018; Rajendran et al., 2025).

While we developed this method to be independent of individual tracking, AntOS includes a built-in colour detection feature that can be used to record the positions of worker groups and a focal individual ant marked with the established colour-marking techniques (Sendova-Franks & Franks, 1993). This functionality could be extended to track multiple individuals within a colony by combining colour detection with additional algorithms such as blob segmentation, k-means algorithm, trained classifier, etc. The number of individuals that can be tracked, will depend on their body size and hence the number of colour dots that can be applied to their body. In the case of *L. niger*, likely only two colour dots of large enough size can be placed on each ant, which given with the limited range of colours that can be differentially recorded in the system (approx. 4 – 5) limits the number of traceable colour coded individuals to approx. 20 in our system. Also, increasing the number of tracked individuals inevitably slows frame processing. The current processing time of 0.5 s per frame could extend to several seconds under higher tracking loads.

As showcased in our experimental study, AntOS already provides a powerful tool to observe and analyse long-term temporal and spatial collective activity, including the emergence of subtle changes and reaction to disturbance over time. As such, we consider the framework developed in this study to be a versatile analysis tool allowing in-depth analysis of otherwise hard-to-grasp noisy data of behavioural patterns of social insect colonies or other insect groups as a whole and to pick up gradual changes over a long-term period. Importantly, it does not require tagging of individuals nor does it rely on the expression of very clear behavioural changes. Due to its simplicity of hardware building blocks and low requirements, the system is easily scalable as it allows parallel, continuous observation of a high number of colonies. It can therefore be built up as a high-throughput system to simultaneously analyse high replicate

numbers of colonies over long periods for both their temporal and spatial collective activity patterns. Our system can be used to follow the colony development and growth as a direct estimate for fitness, and how it is influenced by different experimental conditions.

Although several components of the framework were implemented with easy-to-use GUI interfaces, its current implementation requires a degree of technical expertise. Users need familiarity with Python, designing 3D parts and connecting simple electronics to Raspberry Pi devices. However, these requirements have become increasingly manageable as user-friendly programming support (e.g. AI-assisted coding) and widely available modular maker technologies continue to lower the barrier for researchers without strong engineering backgrounds. We therefore see the operability of such systems steadily improving alongside these broader developments, improving the usability of such low-threshold accessible and low-cost technology for future behavioural studies.

AUTHOR CONTRIBUTIONS

Jinook Oh and Sylvia Cremer conceived the project together. Jinook Oh designed and built the hardware and software, collected and analysed the data. Jinook Oh led the writing of the manuscript; Sylvia Cremer contributed critically to the drafts and both authors gave final approval for publication.

ACKNOWLEDGEMENTS

We thank Harikrishnan Rajendran for discussion. This project has received funding from the European Research Council (ERC) under the European Union's Horizon 2020 Research and Innovation Programme (grant agreement No. 771402; EPIDEMICSonCHIP to S.C.). Open Access funding provided by Institute of Science and Technology Austria/KEMÖ.

CONFLICT OF INTEREST STATEMENT

The authors declare no potential conflict of interest.

PEER REVIEW

The peer review history for this article is available at https://www.webofscience.com/api/gateway/wos/peer-review/10.1111/2041-210x.70277.

DATA AVAILABILITY STATEMENT

Data available via https://doi.org/10.5281/zenodo.16893940 (Oh, 2025), and the code is available at Github, https://github.com/jinook0707/CremerGroupApp.

ORCID

Jinook Oh https://orcid.org/0000-0001-7425-2372

REFERENCES

Ardekani, R., Biyani, A., Dalton, J. E., Saltz, J. B., Arbeitman, M. N., Tower, J., Nuzhdin, S., & Tavaré, S. (2013). Three-dimensional tracking and behaviour monitoring of multiple fruit flies. *Journal of the Royal Society, Interface*, *10*(78), 20120547.

Balch, T., Khan, Z., & Veloso, M. (2001). Automatically tracking and analyzing the behavior of live insect colonies. In *Proceedings of the fifth International Conference on Autonomous agents* (pp. 521–528). ACM.

Bhatkar, A., Whitcomb, W., Buren, W., Callahan, P., & Carlysle, T. (1972). Confrontation behavior between *Lasius neoniger* (Hymenoptera: Formicidae) and the imported fire ant. *Environmental Entomology*, *1*(3), 274–279.

Blut, C., Crespi, A., Mersch, D., Keller, L., Zhao, L., Kollmann, M., Schellscheidt, B., Fülber, C., & Beye, M. (2017). Automated computer-based detection of encounter behaviours in groups of honeybees. *Scientific Reports*, *7*(1), 17663.

Boenisch, F., Rosemann, B., Wild, B., Dormagen, D., Wario, F., & Landgraf, T. (2018). Tracking all members of a honey bee colony over their lifetime using learned models of correspondence. *Frontiers in Robotics and AI*, *5*, 35.

Boi, S., Couzin, I. D., Buono, N. D., Franks, N., & Britton, N. (1999). Coupled oscillators and activity waves in ant colonies. *Proceedings of the Royal Society of London, Series B: Biological Sciences*, *266*(1417), 371–378.

Brahma, A., Mandal, S., & Gadagkar, R. (2018). Emergence of cooperation and division of labor in the primitively eusocial wasp *Ropalidia marginata*. *Proceedings of the National Academy of Sciences of the United States of America*, *115*(4), 756–761.

Brazier, M. A. (1962). The analysis of brain waves. *Scientific American*, *206*(6), 142–155.

Castelo, J., Pinto, H. S., Bernardino, A., & Baylina, N. (2020). Video based live tracking of fishes in tanks. In *Image analysis and recognition: 17th International Conference, ICIAR 2020, Póvoa de Varzim, Portugal, June 24–26, 2020, proceedings, part I 17* (pp. 161–173). Springer.

Cole, B. J. (1991). Short-term activity cycles in ants: Generation of periodicity by worker interaction. *The American Naturalist*, *137*(2), 244–259.

Cole, B. J., & Trampus, F. I. (1999). Activity cycles in ant colonies: Worker interactions and decentralized control. In *Information processing in social insects* (pp. 289–307). Springer.

Cremer, S. (2019). Social immunity in insects. *Current Biology*, *29*(11), R458–R463.

Currie, C. R., & Stuart, A. E. (2001). Weeding and grooming of pathogens in agriculture by ants. *Proceedings of the Royal Society of London. Series B: Biological Sciences*, *268*(1471), 1033–1039.

Czechowski, W., Radchenko, A., Czechowska, W., & Vepsäläinen, K. (2012). *The ants of Poland with reference to the myrmecofauna of Europe*. Natura Optima Dux Foundation.

Dankert, H., Wang, L., Hoopfer, E. D., Anderson, D. J., & Perona, P. (2009). Automated monitoring and analysis of social behavior in Drosophila. *Nature Methods*, *6*(4), 297–303.

Depickère, S., Fresneau, D., & Deneubourg, J.-L. (2004). A basis for spatial and social patterns in ant species: Dynamics and mechanisms of aggregation. *Journal of Insect Behavior*, *17*(1), 81–97.

Doronina-Amitonova, L., Fedotov, I., Fedotov, A. B., Anokhin, K. V., & Zheltikov, A. M. (2015). Neurophotonics: Optical methods to study and control the brain. *Physics-Uspekhi*, *58*(4), 345.

Dunn, J. D., Hodapp, D., Menzel, F., & Kohlmeier, P. (2024). Larval chemical cues induce rapid changes in foraging preferences of ant workers (Hymenoptera: Formicidae). *Myrmecological News*, *34*, 71–79.

Ferral, N., Holloway, K., Li, M., Yin, Z., & Hou, C. (2018). Heterogeneous activity causes a nonlinear increase in the group energy use of ant workers isolated from queen and brood. *Insect Science*, *25*(3), 487–498.

Fujioka, H., Abe, M. S., Fuchikawa, T., Tsuji, K., Shimada, M., & Okada, Y. (2017). Ant circadian activity associated with brood care type. *Biology Letters*, *13*(2), 20160743.

Gal, A., Saragosti, J., & Kronauer, D. J. (2020). anTraX, a software package for high-throughput video tracking of color-tagged insects. *eLife*, *9*, e58145.

Geffre, A. C., Gernat, T., Harwood, G. P., Jones, B. M., Morselli Gysi, D., Hamilton, A. R., Bonning, B. C., Toth, A. L., Robinson, G. E., & Dolezal, A. G. (2020). Honey bee virus causes context-dependent changes in host social behavior. *Proceedings of the National Academy of Sciences of the United States of America*, *117*(19), 10406–10413.

Gell-Mann, M. (2002). What is complexity? In *Complexity and industrial clusters: Dynamics and models in theory and practice* (pp. 13–24). Springer.

Giancardo, L., Sona, D., Huang, H., Sannino, S., Managò, F., Scheggia, D., Papaleo, F., & Murino, V. (2013). Automatic visual tracking and social behaviour analysis with multiple mice. *PLoS One*, *8*(9), e74557.

Harris, C. R., Millman, K. J., van der Walt, S. J., Gommers, R., Virtanen, P., Cournapeau, D., Wieser, E., Taylor, J., Berg, S., Smith, N. J., Kern, R., Picus, M., Hoyer, S., van Kerkwijk, M. H., Brett, M., Haldane, A., del Río, J. F., Wiebe, M., Peterson, P., … Oliphant, T. E. (2020). Array programming with NumPy. *Nature*, *585*(7825), 357–362. https://doi.org/10.1038/s41586-020-2649-2

Hölldobler, B., & Wilson, E. O. (1990). *The ants*. Harvard University Press.

Kauffman, S. A. (1995). *At home in the universe: The search for laws of self-organization and complexity*. Oxford University Press.

Kays, R., Davidson, S. C., Berger, M., Bohrer, G., Fiedler, W., Flack, A., Hirt, J., Hahn, C., Gauggel, D., Russell, B., Kölzsch, A., Lohr, A., Partecke, J., Quetting, M., Safi, K., Scharf, A., Schneider, G., Lang, I., Schaeuffelhut, F., … Wikelski, M. (2022). The Movebank system for studying global animal movement and demography. *Methods in Ecology and Evolution*, *13*(2), 419–431.

Koto, A., Tamura, M., Wong, P. S., Aburatani, S., Privman, E., Stoffel, C., Crespi, A., McKenzie, S. K., La Mendola, C., Kay, T., & Keller, L. (2023). Social isolation shortens lifespan through oxidative stress in ants. *Nature Communications*, *14*(1), 5493.

Leckie, L., Andon, M. S., Bruce, K., & Stroeymeyt, N. (2025). Architectural immunity: Ants alter their nest networks to prevent epidemics. *Science*, *390*(6770), 266–271.

Leclerc, J.-B., Pinto Silva, J., & Detrain, C. (2018). Impact of soil contamination on the growth and shape of ant nests. *Royal Society Open Science*, *5*(7), 180267.

Lei, Y., Jaleel, W., Shahzad, M. F., Ali, S., Azad, R., Ikram, R. M., Ali, H., Ghramh, H. A., Khan, K. A., Qiu, X., Faisal Shahzad, M., Muhammad Ikram, R., Ali Khan, K., He, Y., & Lyu, L. (2021). Effect of constant and fluctuating temperature on the circadian foraging rhythm of the red imported fire ant, *Solenopsis invicta* Buren (Hymenoptera: Formicidae). *Saudi Journal of Biological Sciences*, *28*(1), 64–72.

Liu, S., Han, L., Liu, X., Ren, J., Wang, F., & Lin, Y. (2023). FishMOT: A simple and effective method for fish tracking based on IoU matching. arXiv Preprint arXiv:2309.02975.

Mersch, D. P., Crespi, A., & Keller, L. (2013). Tracking individuals shows spatial fidelity is a key regulator of ant social organization. *Science*, *340*(6136), 1090–1093.

Mildner, S., & Roces, F. (2017). Plasticity of daily behavioral rhythms in foragers and nurses of the ant *Camponotus rufipes*: Influence of social context and feeding times. *PLoS One*, *12*(1), e0169244.

Miller, N. D., Yoder, T. J., Manoukis, N. C., Carvalho, L. A., & Siderhurst, M. S. (2022). Harmonic radar tracking of individual melon flies, *Zeugodacus cucurbitae*, in Hawaii: Determining movement parameters in cage and field settings. *PLoS One*, *17*(11), e0276987.

Napoli, M., Sipahi, R., & Porfiri, M. (2025). The role of colony size on activity rhythms of ants. *Journal of Theoretical Biology*, *617*, 112286.

Noldus, L. P., Spink, A. J., & Tegelenbosch, R. A. (2002). Computerised video tracking, movement analysis and behaviour recognition in insects. *Computers and Electronics in Agriculture*, *35*(2–3), 201–227.

Ogawa, S., Lee, T.-M., Kay, A. R., & Tank, D. W. (1990). Brain magnetic resonance imaging with contrast dependent on blood oxygenation. *Proceedings of the National Academy of Sciences of the United States of America*, *87*(24), 9868–9872.

Oh, J. (2025). Data for ALTAA: Analysis of long-term activity patterns in ant colonies. Version v1. https://doi.org/10.5281/zenodo.16893940

Oskui, S. M., Diamante, G., Liao, C., Shi, W., Gan, J., Schlenk, D., & Grover, W. H. (2016). Assessing and reducing the toxicity of 3D-printed parts. *Environmental Science & Technology Letters*, *3*(1), 1–6.

Papadopoulou, M., Fürtbauer, I., O'Bryan, L. R., Garnier, S., Georgopoulou, D. G., Bracken, A. M., Christensen, C., & King, A. J. (2023). Dynamics of collective motion across time and species. *Philosophical Transactions of the Royal Society, B: Biological Sciences*, *378*(1874), 20220068.

Phillips, I. D., & Willis, C. K. (2005). Defensive behavior of ants in a mutualistic relationship with aphids. *Behavioral Ecology and Sociobiology*, *59*, 321–325.

Popp, S., & Dornhaus, A. (2023). Ant colonies explore novel environments with more slower, curvier walks, particularly near the nest. *Insectes Sociaux*, *70*(4), 463–474.

Pull, C. D., Ugelvig, L. V., Wiesenhofer, F., Grasse, A. V., Tragust, S., Schmitt, T., Brown, M. J., & Cremer, S. (2018). Destructive disinfection of infected brood prevents systemic disease spread in ant colonies. *eLife*, *7*, e32073.

Quevillon, L. E., Hanks, E. M., Bansal, S., & Hughes, D. P. (2015). Social, spatial and temporal organization in a complex insect society. *Scientific Reports*, *5*(1), 13393.

Rajendran, H., Weinberger, R., Fonio, E., & Feinerman, O. (2025). Colony demographics shape nest construction in *Camponotus fellah* ants. *eLife*, *13*, e100706.

Richardson, T. O., Liechti, J. I., Stroeymeyt, N., Bonhoeffer, S., & Keller, L. (2017). Short-term activity cycles impede information transmission in ant colonies. *PLoS Computational Biology*, *13*(5), e1005527.

Robinson, E. J., Richardson, T. O., Sendova-Franks, A. B., Feinerman, O., & Franks, N. R. (2009). Radio tagging reveals the roles of corpulence, experience and social information in ant decision making. *Behavioral Ecology and Sociobiology*, *63*, 627–636.

Scharf, I., Pamminger, T., & Foitzik, S. (2011). Differential response of ant colonies to intruders: Attack strategies correlate with potential threat. *Ethology*, *117*(8), 731–739.

Sclocco, A., Ong, S. J. Y., Aung, S. Y. P., & Teseo, S. (2020). Integrating real-time data analysis into automatic tracking of social insect behavior. bioRxiv, 2020–11.

Sendova-Franks, A., & Franks, N. R. (1993). Task allocation in ant colonies within variable environments (a study of temporal polyethism: Experimental). *Bulletin of Mathematical Biology*, *55*, 75–96.

Sendova-Franks, A. B., & Franks, N. R. (1995). Spatial relationships within nests of the ant *Leptothorax unifasciatus* (*Latr.*) and their implications for the division of labour. *Animal Behaviour*, *50*(1), 121–136.

Shen, M., Szyszka, P., Deussen, O., Galizia, C. G., & Merhof, D. (2015). Automated tracking and analysis of behavior in restrained insects. *Journal of Neuroscience Methods*, *239*, 194–205.

Siehler, O., Wang, S., & Bloch, G. (2021). Social synchronization of circadian rhythms with a focus on honeybees. *Philosophical Transactions of the Royal Society, B: Biological Sciences*, *376*(1835), 20200342.

Stroeymeyt, N., Grasse, A. V., Crespi, A., Mersch, D. P., Cremer, S., & Keller, L. (2018). Social network plasticity decreases disease transmission in a eusocial insect. *Science*, *362*(6417), 941–945.

Theis, F. J., Ugelvig, L. V., Marr, C., & Cremer, S. (2015). Opposing effects of allogrooming on disease transmission in ant societies. *Philosophical Transactions of the Royal Society, B: Biological Sciences*, *370*(1669), 20140108.

Theraulaz, G., Bonabeau, E., Nicolis, S. C., Solé, R. V., Fourcassié, V., Blanco, S., Fournier, R., Joly, J.-L., Fernández, P., Grimal, A., Dalle, P., & Deneubourg, J.-L. (2002). Spatial patterns in ant colonies. *Proceedings of the National Academy of Sciences of the United States of America*, *99*(15), 9645–9649.

Ulrich, Y., Saragosti, J., Tokita, C. K., Tarnita, C. E., & Kronauer, D. J. (2018). Fitness benefits and emergent division of labour at the onset of group living. *Nature*, *560*(7720), 635–638.

Welch, P. (1967). The use of fast Fourier transform for the estimation of power spectra: A method based on time averaging over short, modified periodograms. *IEEE Transactions on Audio and Electroacoustics*, *15*(2), 70–73.

Wilson, E. O. (1955). *A monographic revision of the ant genus Lasius*. Bulletin of the Museum of Comparative Zoology at Harvard College.

Wilson, E. O., Durlach, N. I., & Roth, L. M. (1958). Chemical releasers of necrophoric behavior in ants. *Psyche: A Journal of Entomology*, *65*, 108–114.

Young, M.-S., Young, C., & Li, Y. (2000). A combined system for measuring animal motion activities. *Journal of Neuroscience Methods*, *95*(1), 55–63.

SUPPORTING INFORMATION

Additional supporting information can be found online in the Supporting Information section at the end of this article.

Appendix A. Costs.

Appendix B. Python files for software of the framework.

Appendix C. Commonly used classes and functions.

Appendix D. Calculating '*proxMCluster*' values.

Appendix E. Fitted exponential decay parameters (A_0, k, half-life) for each colony's activity response to disturbance.

How to cite this article: Oh, J., & Cremer, S. (2026). ALTAA: Analysis of long-term activity patterns in ant colonies. *Methods in Ecology and Evolution*, *17*, 1218–1234. https://doi.org/10.1111/2041-210x.70277